Dissipative acceptor-valence-band tunnelling in GaAs:C_{As}

1995 J. Phys.: Condens. Matter 7 8967

(http://iopscience.iop.org/0953-8984/7/47/016)

J. Phys.: Condens. Matter 7 (1995) 8967–8977. Printed in the UK

Dissipative acceptor–valence-band tunnelling in GaAs:C_{As}

A Dargys†, Š Kudžmauskas‡ and S Žurauskas†

† Semiconductor Physics Institute, A Goštauto 11, 2600 Vilnius, Lithuania
‡ Institute of Theoretical Physics and Astronomy, A Goštauto 12, 2600 Vilnius, Lithuania

Received 31 May 1995

Abstract. Field ionization properties of shallow carbon acceptors in MBE GaAs, where thermal lattice vibrations have an effect on the hole emission rate, are presented. The excited energy levels of the carbon atom are relatively far from the ground level; therefore, it appeared possible to observe pure phonon-assisted tunnelling of a hole from a single (ground) level over a wide temperature range, from 4.2 K to 22 K. Experimental results are interpreted using a multiphonon field ionization model that takes into account the interaction of acoustic phonons with a localized centre via deformation and piezoelectric potentials. In the temperature range considered, the influence of the deformation potential is found to predominate over the piezoelectric one.

1. Introduction

Dissipation may either suppress or enhance the quantum mechanical tunnelling rate. In semiconductors, due to intense charge-carrier interaction with lattice vibrations, enhancement is usually observed [1–9]. On the other hand, in a current-biased Josephson junction shunted with a normal-metal resistor, reduction of the tunnelling rate by a factor of about 300 due to effect of dissipation is observed [10, 11]. Most of the results on tunnelling in semiconductors published hitherto are concerned with optical-phonon-assisted tunnelling (PAST) through potential barriers formed by p–n junctions, heterobarriers or oxide layers [1]. The PAST mechanism is important in the field ionization of point centres too [2–8]. Earlier investigations [2–8] were devoted to deep impurities, in which the energetic distance between the ground and excited impurity levels is much larger than the optical phonon energy. It was found that the ionization of such centres could be explained by interaction of charge carriers with optical lattice vibrational modes. However, in the case of shallow impurities and low lattice temperatures one expects that coupling to acoustic vibrational modes will predominate, especially when the ionization energy of the impurity centre is much smaller than the optical phonon energy. In our earlier investigations of silicon doped with shallow phosphorus impurities [9], instead of the PAST we observed a different mechanism associated with acoustic phonons, namely, acoustic-phonon-activated tunnelling (PACT). In the PACT process the phosphorus atom at first absorbs acoustic phonon(s), and as a result becomes excited. Only then does it emit an electron through a more transparent potential barrier (see figure 1). The PACT predominates over the PAST if the combined probability of excitation and tunnelling is larger than the probability of tunnelling out of the ground level, level 1. As shown in [9, 12], the slope of the logarithm of the emission rate as a function of the inverse temperature yields the energetic distance between the ground (level 1) and the excited (level 2) energy levels if the PACT process predominates.

0953-8984/95/478967+11$19.50

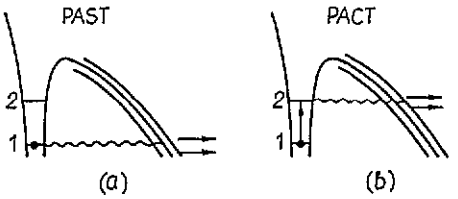

Figure 1. Phonon-assisted (*a*) and phonon-activated (*b*) mechanisms of tunnelling of the charge carrier from ground level 1. The carrier tunnels through the thermally vibrating barrier represented by three lines; as a result its final energy may increase or decrease, as shown by the horizontal arrows.

Below, we present experimental data and theory on the acoustic PAST process. For this purpose we measured the field ionization of shallow carbon acceptors in GaAs as a function of lattice temperature. In carbon atoms the distance between the ground and the first excited levels is large enough that over a wide temperature range only the ground level is populated by holes. According to [12], the PACT in GaAs:C_{As} is expected to become important at lattice temperatures of about 28 K or higher. This investigation may be considered as a continuation of [13], where we studied pure acceptor–valence-band tunnelling dynamics in GaAs:C_{As}.

2. Experiment

The samples were fabricated from the same MBE wafer whose growth procedure was described in [13]. The (100)-oriented wafer consisted of heavily doped n^+-type substrate, a 13 μm thickness layer of the p-GaAs being investigated, and a 0.9 μm p^+-type gate cap layer for contact. The samples used in this study were prepared in a different manner and were of different configurations. After suitable metallization of both wafer faces, mesas of area 0.12 mm^2 were etched out on the p^+ side, and then the substrate was cleaved to samples of about 1 mm^2 area (see the inset in figure 2). A whisker lightly applied to the metallized p^+ cap layer served as a gate electrode. The acceptor concentration in the p layer was about 5×10^{14} cm^{-3}.

The influence of acoustic phonons on the acceptor field ionization dynamics was investigated with the help of a transient tunnelling spectrometer [14]. The reverse-biased pn^+ junction served as a blocking contact while the heavily doped p^+ region served as a collecting contact. The acceptor–valence-band tunnelling occurred in the p layer (see figure 1 in [13]).

In figure 2 there is shown a fast (lying in a nanosecond time-range), ramped voltage over the sample and the resulting transient current at liquid helium temperature. The current spectrum observed with the present mesa-shaped samples coincides with that observed in [13] for platelet-shaped samples; the area of the latter was larger by nearly an order of magnitude. The similarity of the spectra means that in all cases surface effects are negligible and that the sample geometrical capacitance and spectrometer response time do not influence the experimental results. In figure 2 the plateau in the current density is due to charging to about 1 pF sample geometrical capacitance. The tunnelling current density J_t, which is superimposed on the plateau current J_c, consists of two peaks. As demonstrated in [13], the first peak is associated with field ionization of the substitutional carbon acceptor C_{As} and the second, not so well-resolved peak at about 25 ns is associated with field ionization of the acceptor complex d_n [15] that is frequently encountered in MBE-grown layers.

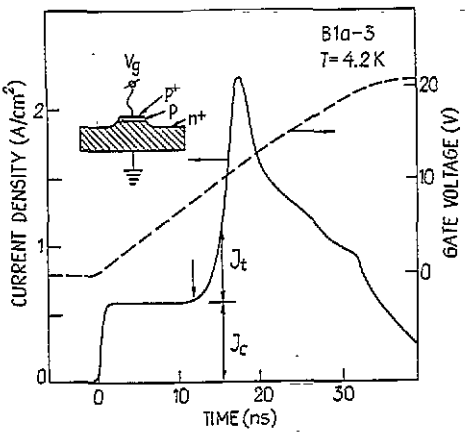

Figure 2. A typical transient current density through and voltage ramp over the mesa-shaped p-GaAs sample B1a-3 (see the inset) at 4.2 K. The vertical arrow indicates the moment when $F = 6$ kV cm^{-1}.

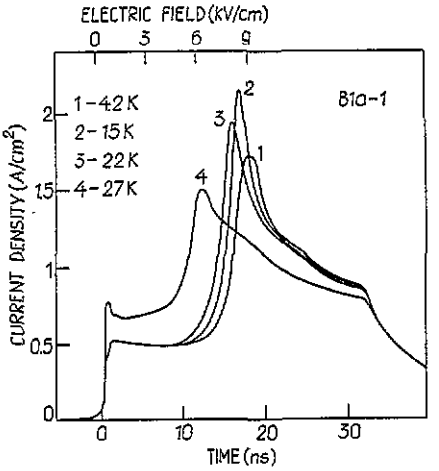

Figure 3. Evolution of the current spectrum with the lattice temperature for mesa-shaped sample B1a-1. The upper scale shows an average electric field in the p region. 1: $T = 4.2$ K; 2: 15 K; 3: 22 K; 4: 27 K.

Figure 3 shows a typical overall view of the current spectrum in mesa-shaped samples at four fixed lattice temperatures. At higher temperatures, in the range $4.2 < T < 22$ K, the leading edge is initiated by ionization of carbon atoms and shifts to earlier times, or equivalently to lower electric fields, when the lattice temperature is raised. This is associated with the participation of phonons in the tunnelling process. In the above temperature range, thermal free holes are absent in the valence band. At $T > 22$ K the presence of thermal holes in the valence band and on the upper acceptor levels (in the spectrum such holes give rise to a narrow peak at the beginning of the ramp and excess current in the interval 0–10 ns) severely distorts the shape of the main tunnelling pulse. In this study all measurements are limited to the temperature range where the influence of thermal free and excited holes on the hole tunnelling dynamics from the ground level is unimportant.

The overall shape of the spectrum depends on the space charge that develops near the pn^+ junction during the voltage ramping. As shown in [9] and especially in [16] at the leading edge, where the current is rising exponentially, the distortions of the electric field due to space charge in the p region are small and can be neglected. Then, the tunnelling current in the leading edge can be described by the formula

$$J_t \approx N^0 \frac{ed(1 - l/d)^2}{2\tau_t} \tag{1}$$

where e is the elementary charge, d is the total width of the p region and l is the width of depletion layer caused by pn^+ junction. N^0 is the neutral carbon concentration. It should be noted that in (1) the tunnelling time τ_t is a function of instantaneous electric field strength F. Since our measuring time-scale is long in comparison with the internal atomic time-scale (the Bohr period), adopting the instantaneous electric field approximation in (1) is fully justified. Experimentally, this point has been considered in [13], where it is shown that the critical electric field, at which the fast leading edge appears, is independent of the ramp rate.

To find a variation of the tunnelling rate (the inverse of τ_t) with the lattice temperature,

the transient tunnelling spectrometer [14] was set in the following measurement regime. The sweeping mode of the sampling oscilloscope, on whose screen the total transient current J is usually observed, was switched off, and the current gating was fixed at the beginning of the leading edge of the tunnelling current pulse, as shown by the vertical arrow in figure 2. Then, the sample temperature was raised slowly by passing a DC current through a sample heater. In this regime it appeared possible to detect very small changes in the tunnelling current $J_t = J - J_C$ when the sample temperature was raised or lowered.

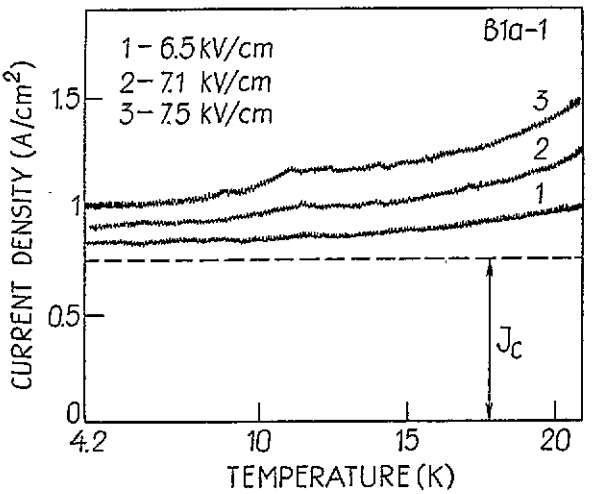

Figure 4. The current density versus the lattice temperature at three electric field values: $F = 6.5$ kV cm^{-1}, 7.1 kV cm^{-1}, and 7.5 kV cm^{-1}.

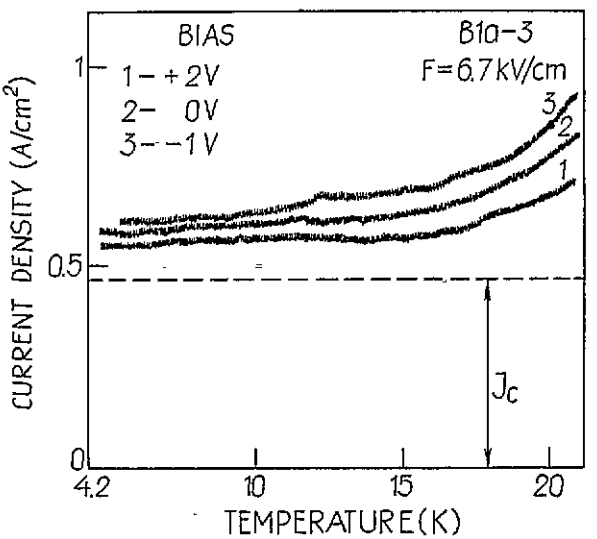

Figure 5. The current density versus the lattice temperature at $F = 6.7$ kV cm^{-1} and three DC bias values: -1 V, 0 V, and 2 V.

Figure 4 shows typical dependencies of J on T at three fixed gating moments, or equivalently three fixed electric field values $F = 6.5$ kV cm^{-1}, 7.1 kV cm^{-1} and

7.5 kV cm^{-1}. Similar dependencies have been observed for all three samples studied. Since the capacitive current J_C practically does not change with lattice temperature, the observed increase of J is associated with an increase of the tunnelling rate with T.

Figure 5 shows J versus T when an additional positive or negative DC bias voltage V_b is applied to the n^+ electrode. V_b increases or decreases the initial width l of the depletion layer in the p region. When $V_b > 0$, the number of neutral acceptors in the p region becomes smaller; as a result, the tunnelling current is proportionally smaller.

3. Theory

Below, we shall calculate the field emission probability when a localized carrier interacts with acoustic vibrations through piezoelectric (PA) and deformation (DA) potentials. Results from the general theory of multiphonon field ionization [2, 17] will be used for this purpose. Within the spherical-energy-band approach, the field ionization rate of the neutral centre is (see formula (26) in [2])

$$W \equiv \frac{1}{\tau_t} = \frac{eF}{2(2m^*E_i)^{1/2}} \exp\left\{-\frac{4}{3}\frac{(2m^*)^{1/2}}{eF\hbar}E_i^{3/2}\right\} \times \exp\left\{\sum_{\nu q}\left|\frac{\Delta_\nu(q)}{\hbar\omega_\nu(q)}\right|^2\left[\exp\left(-\frac{p_i\hbar\omega_\nu(q)}{eF\hbar}\right)-1\right]\right\} \times \exp\left\{\sum_{\nu q}\bar{n}_{\nu q}\left|\frac{\Delta_\nu(q)}{\hbar\omega_\nu(q)}\right|^2\left[\exp\left(\frac{p_i\hbar\omega_\nu(q)}{eF\hbar}\right)+\exp\left(-\frac{p_i\hbar\omega_\nu(q)}{eF\hbar}\right)-2\right]\right\}. \tag{2}$$

Here, $p_i = 2(2m^*E_i)^{1/2}$, E_i is the ionization energy of the impurity atom considered, and m^* is the effective mass of an electron (hole). $\omega_\nu(q) = v_\nu \cdot q$ describes the dispersion law of acoustic phonons with wave vector q and velocity v_ν, where $\nu = l$ for longitudinal and $\nu = t_1$ or t_2 for two transverse phonon polarizations. $\bar{n}_{\nu q}$ is the average phonon number:

$$\bar{n}_{\nu q} = \left[\exp\left(\frac{\hbar\omega_\nu(q)}{kT}\right)-1\right]^{-1}. \tag{3}$$

$\Delta_\nu(q)$ describes the interaction of the bound carrier with the acoustic mode (νq) in the adiabatic approximation [2]. The electron–phonon interaction is characterized by the Hamiltonian

$$H_{ep} = \sum_{\nu q}\left(\alpha_{\nu q}b_{\nu q}e^{iq\cdot r} + \alpha^*_{\nu q}b^+_{\nu q}e^{-iq\cdot r}\right) \tag{4}$$

where $b_{\nu q}$ ($b^+_{\nu q}$) is the annihilation (creation) operator of the (νq)-type phonon and $\alpha_{\nu q}$ is the electron–phonon interaction constant. The electron–phonon interaction in (2) is described by

$$|\Delta_\nu(q)|^2 = |\alpha_{\nu q}|^2|\langle e^{iq\cdot r}\rangle_b|^2 \tag{5}$$

where the term with the exponent is the coherence length of the bound electron (hole) that is characterized by the wave function $\varphi_b(r)$:

$$\langle e^{iq\cdot r}\rangle_b = \int dr\ |\varphi_b(r)|^2 e^{iq\cdot r}. \tag{6}$$

Two extreme forms of φ_i are assumed below. In the first, we shall use the wave function that corresponds to deep δ-type impurity:

$$\varphi_\delta(r) = \left(\frac{\kappa}{2\pi}\right)^{1/2} \frac{\exp(-\kappa r)}{r} \qquad \kappa = \frac{\sqrt{2m^* E_i}}{\hbar}. \tag{7}$$

Such a wave function has been used by Lucovsky [18] to obtain the photoionization cross section for deep impurities and by one of us [2] in the study of the optical PAST process. A more general form of (7) was also used by Makram-Ebeid and Lannoo in optical PAST studies [5]. In the second, the impurity wave function is assumed to be hydrogenic:

$$\varphi_H(r) = \frac{1}{\sqrt{\pi} a_B^{3/2}} \exp(-r/a_B) \tag{8}$$

where a_B is the Bohr radius. The form (8) is more appropriate for shallow impurities. In the latter case the factor $eF/2(2m^*E_i)^{1/2}$ before the exponents in (2) is to be replaced by $16E_i^2/eF\hbar a_B$.

3.1. Piezoelectric interaction

In crystals with zincblende structure the interaction Hamiltonian (4) is [19]

$$H_{ep}^{PA} = -\frac{\bar{e}e_{14}}{\varepsilon_0\varepsilon_r} \sum_{\nu q} \left(\frac{\hbar}{2NM\omega_\nu(q)}\right)^{1/2} \times \left\{2\mathrm{i}\frac{1}{q^2+q_0^2}(a_{\nu x}q_y q_z + a_{\nu y}q_x q_z + a_{\nu z}q_x q_y) b_{\nu q} \mathrm{e}^{\mathrm{i}q\cdot r} + \mathrm{cc}\right\}. \tag{9}$$

Here, $\bar{e}$ is the charge of an electron or hole with a suitable sign, e_{14} is the piezoelectric coefficient, ε_0 is the electrical constant, ε_r is the relative lattice permittivity, N is the number of elementary cells, M is the mass of the elementary cell, q_0 is the inverse screening radius, and $a_{\nu i}$ is the projection of the unit polarization vector, due to displacement of the lattice, on the ith crystallographic axis. Then, the coherence length (6) for deep and shallow impurities becomes

$$\langle \mathrm{e}^{\mathrm{i}q\cdot r}\rangle_\delta = (2\kappa/q)\arctan(q/2\kappa) \tag{10}$$

$$\langle \mathrm{e}^{\mathrm{i}q\cdot r}\rangle_H = 1/(1+q^2a_B^2/4)^2. \tag{11}$$

By taking into account (3)–(6) and (9)–(11), it is easy to find the quantity $|\Delta_\nu(q)/\hbar\omega_\nu(q)|^2$. After insertion of the latter into (2) and changing summation to integration in spherical coordinates:

$$\sum_q \longrightarrow \frac{N}{\Omega_B}\int_0^{q_D} q^2\,\mathrm{d}q \int_0^{2\pi}\mathrm{d}\varphi \int_{-1}^{1}\mathrm{d}\cos\vartheta \tag{12}$$

one will finally find the tunnelling rate. In (12) Ω_B is the volume of the first Brillouin zone, and q_D (the Debye wavevector) is defined by $\frac{4}{3}\pi q_D^3 = \Omega_B$. In the calculation the quantity

$$I_\nu = (a_{\nu x}q_y q_z + a_{\nu y}q_x q_z + a_{\nu z}q_x q_y)^2 \tag{13}$$

from the Hamiltonian (9) appears. We shall use the same average polarization vectors as in [19]. Then, for longitudinal and transverse phonons one has, respectively,

$$\bar{I}_l = q^{-2}(3q_x q_y q_z)^2 \tag{14}$$

and

$$\bar{I}_t = q_x^2q_y^2 + q_y^2q_z^2 + q_z^2q_x^2 - q^{-2}(3q_x q_y q_z)^2. \tag{15}$$

Then, after integration over φ and $\cos\vartheta$, the final expression for the rate of tunnelling out of the δ-type centre becomes

$$W_\delta^{PA} = \frac{eF}{2(2m^*E_i)^{1/2}} \exp\left[-\frac{4}{3}\frac{(2m^*)^{1/2}E_i^{3/2}}{eF\hbar}\right] \times \exp\left[\int_0^{q_D} \mathrm{d}q \frac{q\kappa^2 \arctan^2(q/2\kappa)}{(q^2+q_0^2)^2}(A_{\delta.l}D_l + A_{\delta.t}D_t + A_{\delta.l}Q_l + A_{\delta.t}Q_t)\right] \tag{16}$$

and that out of the hydrogenic centre becomes

$$W_H^{PA} = \frac{16E_i^2}{eF\hbar a_B} \exp\left[-\frac{4}{3}\frac{(2m^*)^{1/2}E_i^{3/2}}{eF\hbar}\right] \exp\left[\int_0^{q_D} \mathrm{d}q \frac{q^3}{(q^2+q_0^2)^2(1+a_B^2q^2/4)^4} \times (A_{H.l}D_l + A_{H.t}D_t + A_{H.l}Q_l + A_{H.t}Q_t)\right] \tag{17}$$

where

$$D_\nu = \exp(-q/q_{F.\nu}) - 1 \tag{18}$$

$$Q_\nu = [\exp(q/q_{F.\nu}) + \exp(-q/q_{F.\nu}) - 2]/[\exp(q/q_{T.\nu}) - 1] \tag{19}$$

$$q_{F.\nu} = \frac{eF\hbar}{2(2m^*E_i)^{1/2}\hbar v_\nu} \qquad q_{T.\nu} = \frac{kT}{\hbar v_\nu} \qquad \nu = \mathrm{l}, \mathrm{t} \tag{20}$$

$$A_{\delta.\nu} = \frac{\pi\beta_{\delta.\nu}\bar{e}^2e_{14}^2}{(\varepsilon_0\varepsilon_r)^2\hbar v_\nu^3 M\Omega_B} \qquad \beta_{\delta.l} = \frac{96}{35} \qquad \beta_{\delta.t} = \frac{128}{35} \tag{21}$$

$$A_{H.\nu} = \frac{\pi\beta_{H.\nu}\bar{e}^2e_{14}^2}{(\varepsilon_0\varepsilon_r)^2\hbar v_\nu^3 M\Omega_B} \qquad \beta_{H.l} = \frac{24}{35} \qquad \beta_{H.t} = \frac{32}{35}. \tag{22}$$

3.2. Deformation potential interaction

For simple energy bands characterized by spherical energy surfaces, only longitudinal phonons give contributions to the deformation potential interaction [20]:

$$H_{ep}^{DA} = -\mathrm{i}E_1 \sum_q q \left(\frac{\hbar}{2NM\omega_l(q)}\right)^{1/2} (b_q \mathrm{e}^{\mathrm{i}q\cdot r} + \mathrm{cc}) \tag{23}$$

where E_1 is the acoustic deformation potential constant. In exactly the same manner as in section 3.1, one can find the following expression for the rate of tunnelling out of the δ-like centre:

$$W_\delta^{DA} = \frac{eF}{2(2m^*E_i)^{1/2}} \exp\left[-\frac{4}{3}\frac{(2m^*)^{1/2}E_i^{3/2}}{eF\hbar}\right] \times \exp\left[\int_0^{q_D} \frac{\mathrm{d}q}{q} \arctan^2(q/2\kappa)(B_{\delta.l}D_l + B_{\delta.l}Q_l)\right] \tag{24}$$

where

$$B_{\delta.l} = 8\pi E_1^2\kappa^2/\hbar v_l^3 M\Omega_B. \tag{25}$$

The rate of tunnelling out of the hydrogenic centre is

$$W_H^{DA} = \frac{16E_i^2}{eF\hbar a_B}\exp\left[-\frac{4}{3}\frac{(2m^*)^{1/2}E_i^{3/2}}{eF\hbar}\right] \times \exp\left[\int_0^{q_D} \mathrm{d}q\ \frac{q}{(1+a_B^2q^2/4)^4}(B_{H,l}D_l + B_{H,t}Q_t)\right] \tag{26}$$

where

$$B_{H,l} = 4\pi E_1^2/\hbar v_l^3 M\Omega_B. \tag{27}$$

In the above-obtained final expressions (16), (17), (24) and (26) the first exponent describes bare tunnelling. Only the second exponent takes into account the electron–phonon interaction. Here the terms associated with D_ν are corrections due to the dressing of the centre with a phonon field. Only the terms associated with Q_ν take into account the dependence of the tunnelling rate on the lattice temperature. Note that the Q_ν-terms, apart from the lattice temperature, also depend on the electric field.

4. Comparison between experiment and theory; discussion

The formulae obtained with the hydrogenic wave functions will be used in the analysis of the experimental data, because the hydrogenic functions are more suitable for the description of shallow-acceptor ground states. Measured emission rates will be compared with the normalized theoretical ones (17) and (26):

$$R^{PA} \equiv \frac{W_H^{PA}(T)}{W_H^{PA}(0)} = \exp\left[\sum_{\nu=l,t} A_{H,\nu}\int_0^{\Theta/T} \mathrm{d}x\ \frac{Q_\nu x^3}{(x^2+x_0^2)^2(1+a_B^2q_{T,\nu}^2x^2/4)^4}\right] \tag{28}$$

$$R^{DA} \equiv \frac{W_H^{DA}(T)}{W_H^{DA}(0)} = \exp\left[B_{H,l}q_{T,l}^2\int_0^{\Theta/T} \mathrm{d}x\ \frac{Q_l x}{(1+a_B^2q_{T,l}^2x^2/4)^4}\right]. \tag{29}$$

Here, $x = q/q_{T,\nu}$. The integrals are not sensitive to the upper bound; therefore q_D was approximated as $k\Theta/\hbar v_\nu$, where Θ is Debye temperature. Our simple theory neglects the fact that the valence band of GaAs is characterized by two light- and heavy-hole effective masses. The binding energy and Bohr radius a_B of the ground-state wave function are mainly determined by the heavy-hole mass m_h^*, whereas the asymptotic behaviour of the wave function is determined by light-hole mass m_l^* [21]. For this reason the Bohr radius is calculated using m_h^*:

$$a_B = \hbar\Big/\sqrt{2m_h^*E_i} \tag{30}$$

while $q_{F,\nu}$ in (20) is calculated using m_l^*. This is in agreement with our conclusion in [13], where the pure quantum mechanical tunnelling dynamics is found to be better described using m_l^*.

In figures 6 and 7 there are shown normalized emission rates as a function of lattice temperature calculated using (28) and (29) at various electric field values. The parameter values that are typical for GaAs:C_{As} have been used [22]: $\Theta = 300$ K, $E_1 = 8$ eV, $e_{14} = 0.16$ C m^{-2}, $\varepsilon_r = 12.5$, $v_l = 5.2\times10^3$ m s^{-1}, $v_t = 3\times10^3$ m s^{-1}, $\rho = 5.31$ g cm^{-3} ($M\Omega_B = (2\pi)^3\rho$), $E_i = 26$ meV, $m_h^* = 0.59m_0$, $m_l^* = 0.0905m_0$. The value of m_l^* corresponds to the direction of the electric field: $F \parallel \langle 100\rangle$. The screening wave number is taken as $q_0 = 0$.

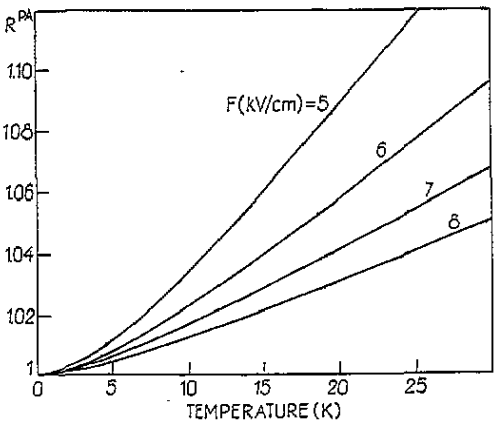

Figure 6. The normalized tunnelling rate, equation (28), for piezoelectric PAST at the electric field values indicated on curves.

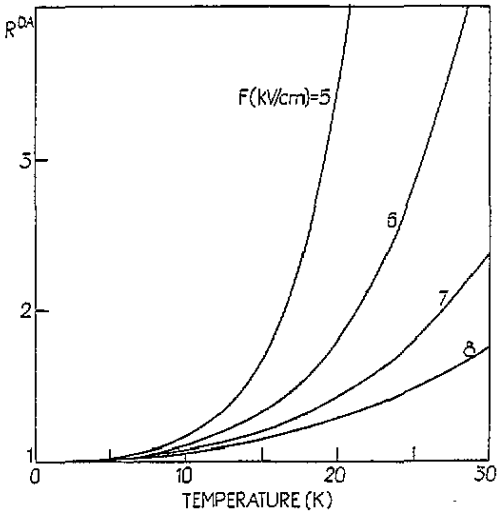

Figure 7. The normalized tunnelling rate, equation (29), for deformation potential PAST at the electric field values indicated on curves.

Some comments concerning the deformation potential value E_1 are indicated. In cubic semiconductors the effect of the deformation potential is described with three constants a, b, and d. According to [23], in GaAs $a = -6.9$ eV, $b = -1.7$ eV and $d = -5.3$ eV. In the present theory, the hole is assumed to interact only via dilation deformation. In real III–V compounds the interaction is also mediated by shear deformation. A necessary combination of a, b and d constants that describes an effective deformation potential E_1 has been derived by Lawaetz (see [24, 25]) in the case of free-hole transport. In calculating the acceptor–valence-band tunnelling the effective deformation potential deduced by Lawaetz has been used. Since in the case of field ionization a different combination of a, b and d may enter the tunnel emission expressions (28) and (29), some uncertainty remains in selecting the E_1-value.

As seen from figures 6 and 7 the interaction of thermal acoustic phonons with the point centre enhances the emission rate in all cases. The ratio of the integrals that appear in (28)

and (29) does not exceed 3 in the temperature and electric field ranges considered; thus, the predominance of the deformation potential interaction over the piezoelectric one is mainly determined by coefficients before the integrals. For our parameter values the ratio of the coefficients is

$$B_{H,l}q_{T,l}^2/A_{H,l} \approx (T\ (\mathrm{K})/3)^2. \tag{31}$$

In figure 8 some of the experimental results from figure 4 are plotted as points and corresponding theoretical curves. Only the strongest—i.e. deformation potential—interaction is taken into account. In GaAs:C_{As}, practically pure quantum mechanical tunnelling occurs at $T = 4.2$ K; thus, comparison of the experimental values normalized to $T = 4.2$ K with the theory is justified. Although experiment and theory give similar trends and order, the measured values are found to be higher in all cases, especially at high lattice temperatures. This may be caused by uncertainties in E_1 and a_B. For example, reduction of the Bohr radius by 10% increases the tunnelling rate by roughly 25%. The same conclusion is drawn from the comparison of experimental and theoretical results, when a DC bias is applied to the sample.

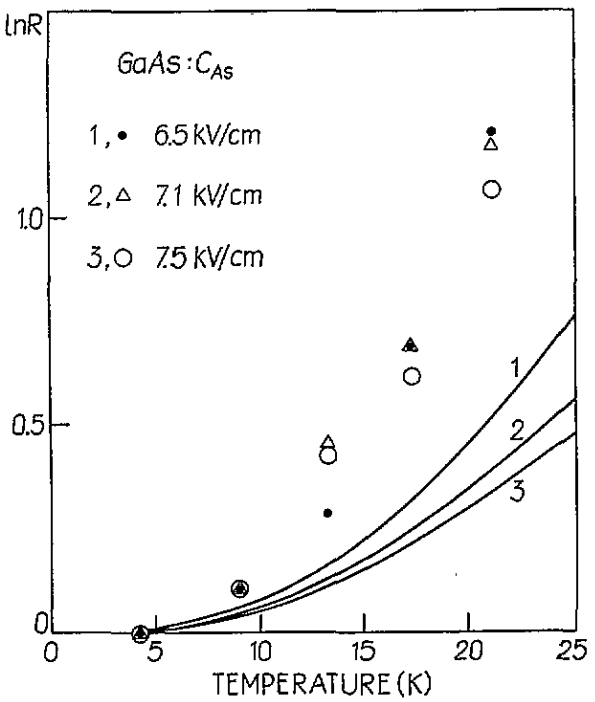

Figure 8. The normalized tunnelling rate versus temperature at three electric field values. The points show experimental values from figure 4, while the lines show the results from the calculation with equation (29). Note that the vertical scale is logarithmic.

In [13] we have been able to detect field emission of electrons from the compensating donors to the GaAs conduction band at about 500 V cm^{-1}. Our PAST model is well adapted to this case. Using the donor activation energy $E_i = 5.7$ meV we have calculated that at $F = 500$ V cm^{-1} the contribution of the PAST to the tunnelling rate makes up about 5% at 4.2 K and 65% at 10 K.

5. Conclusions

The acceptor–valence-band field emission rate in the system GaAs:C_{As} is found to be enhanced by interaction of the carbon acceptor with acoustic thermal vibrations. A comparatively large energetic distance between the ground level (26 meV) and the first excited level (10.8 meV) allowed us to observe a pure PAST process over a wide temperature interval and to neglect the PACT process altogether. Contrary to what is found for the optical PAST process, where the rate of tunnelling emission of a charge carrier out of the deep impurity is observed to increase by many orders of magnitude due to participation of optical phonons [4, 5], we found that the influence of acoustic phonons on the PAST process is comparatively weak. Theoretical analysis shows that at a fixed acceptor ionization energy the acoustical PAST rate is stronger when the wave function of the centre is more localized, i.e. when the Bohr radius is smaller and the centre potential is closer to Dirac's δ-function [17]. Of the two interaction mechanisms considered, we find that the acoustical deformation potential interaction with the carbon acceptor, rather than the piezoelectric interaction, predominates in the temperature range from 4.2 K to 22 K.

Acknowledgments

The authors are grateful to Dr K Bertulis for growing p-GaAs epitaxial layers. The research described in this publication was made possible in part by grants LHR100 and LHV100 from the International Science Foundation.

References

[1] Wolf E L 1985 *Principles of Electron Tunnelling Spectroscopy* (Oxford: Clarendon)
[2] Kudžmauskas Š 1976 *Lietuvos Fiz. Rinkinys* **16** 549 (Engl. Transl. *Sov. Phys. Collection* **16** 31)
[3] Dalidchik F I 1978 *Zh. Eksp. Teor. Fiz.* **74** 472
[4] Makram-Ebeid S 1980 *Appl. Phys. Lett.* **37** 464
[5] Makram-Ebeid S and Lannoo M 1982 *Phys. Rev.* B **25**, 6406
[6] Pipinys P 1985 *Lietuvos Fiz. Rinkinys* **25** 3 (Engl. Transl. *Sov. Phys. Collection* **25** 1)
[7] Karpus V and Perel V I 1986 *Zh. Eksp. Teor. Fiz.* **91** 2319 (Engl. Transl. *Sov. Phys.–JETP* **64** 1376)
[8] Abakumov V N, Karpus V, Perel V I and Yassievich I N 1988 *Fiz. Tverd. Tela* **30** 2498 (Engl. Transl. *Sov. Phys.–Solid State* **30** 1437)
[9] Dargys A, Žurauskienė N and Žurauskas S 1990 *Phys. Status Solidi* b **162** 183
[10] Cleland A N, Martinis J M and Clarke J 1988 *Phys. Rev.* B **37** 5950
[11] Esteve D, Martinis J M, Urbina C, Turlot E and Devoret M H 1989 *Phys. Scr.* T **29** 121
[12] Žurauskienė N, Dargys A and Žurauskas S 1995 *Lietuvos Fiz. Žurnalas* **35** 206
[13] Dargys A and Žurauskas S 1995 *J. Phys.: Condens. Matter* **7** 2133
[14] Dargys A, Žurauskas S and Žurauskienė N 1991 *Appl. Phys.* A **52** 13
[15] Szafranek I, Plano M A, McCollum M J, Stockman S A, Jackson S L, Cheng K Y and Stillman G E 1990 *J. Appl. Phys.* **68** 741
[16] Žurauskas S and Dargys A 1992 *Lietuvos Fiz. Rinkinys* **32** 135 (Engl. Transl. *Lithuanian J. Phys.* **32** 77)
[17] Kudžmauskas Š 1994 *Lietuvos Fiz. Žurnalas* **34** 519 (Engl. Transl. *Lithuanian J. Phys.* **34** 445)
[18] Lucovsky G 1965 *Solid State Commun.* **3** 299
[19] Ridley B K 1982 *Quantum Processes in Semiconductors* (Oxford: Clarendon) ch 3
[20] Bonch-Bruevich V L and Kalashnikov S G 1977 *Semiconductor Physics* (Moscow: Nauka) ch 14
[21] Shklovskii B I and Efros A L 1979 *Electronic Properties of Doped Semiconductors* (Moscow: Nauka) ch 1
[22] Dargys A and Kundrotas J 1994 *Handbook on Physical Properties of Ge, Si, GaAs and InP* (Vilnius: Science and Encyclopedia)
[23] Pfeffer P, Gorczyca I and Zawadzki W 1984 *Solid State Commun.* **51** 179
[24] Lawaetz P 1968 *Phys. Rev.* **174** 867
[25] Wiley J D 1975 *Semicond. Semimet.* **10** 91